

ELM: Embedding and Logit Margins for Long-Tail Learning

Wittawat Jitkrittum, Aditya Krishna Menon, Ankit Singh Rawat, Sanjiv Kumar
 {wittawat, adityakmenon, ankitsrawat, sanjivk}@google.com

Google, New York, USA

April 29, 2022

Abstract

Long-tail learning is the problem of learning under skewed label distributions, which pose a challenge for standard learners. Several recent approaches for the problem have proposed enforcing a suitable margin in logit space. Such techniques are intuitive analogues of the guiding principle behind SVMs, and are equally applicable to linear models and neural models. However, when applied to neural models, such techniques do not explicitly control the geometry of the learned embeddings. This can be potentially sub-optimal, since embeddings for tail classes may be diffuse, resulting in poor generalization for these classes. We present Embedding and Logit Margins (ELM), a unified approach to enforce margins in logit space, and regularize the distribution of embeddings. This connects losses for long-tail learning to proposals in the literature on metric embedding, and contrastive learning. We theoretically show that minimising the proposed ELM objective helps reduce the generalisation gap. The ELM method is shown to perform well empirically, and results in tighter tail class embeddings.

1 Introduction

Practical classification problems often possess skewed label distributions, which pose a challenge for standard learners. This problem of learning under *class imbalance* [Kubat et al., 1997, Chawla et al., 2002, He and Garcia, 2009], or *long-tail learning*, has received renewed interest in the context of neural models [Van Horn and Perona, 2017, Buda et al., 2017, Liu et al., 2019]. Successful approaches to the problem include modifying the training data (e.g., by up- or down-sampling different labels [Kubat and Matwin, 1997, Chawla et al., 2002, Wallace et al., 2011, Mikolov et al., 2013, Mahajan et al., 2018, Yin et al., 2019, Zhang et al., 2019]), modifying the classification rule (e.g., by applying varying thresholds for the different classes [Fawcett and Provost, 1996, Provost, 2000, Maloof, 2003, King and Zeng, 2001, Collell et al., 2016]), and modifying the loss function (e.g., by penalising errors on rare labels more strongly [Zhang et al., 2017, Cui et al., 2019, Cao et al., 2019, Tan et al., 2020, Jamal et al., 2020, Ren et al., 2020, Wu et al., 2020, Menon et al., 2021, Samuel and Chechik, 2021, Kini et al., 2021, Wang et al., 2021a]).

Our interest in this paper is in the latter class of loss modification methods. These have garnered particular interest of late, with several recent works [Cao et al., 2019, Tan et al., 2020, Ren et al., 2020, Menon et al., 2021, Kini et al., 2021, Wang et al., 2021a] establishing the value of enforcing *asymmetric logit margins*. Such techniques are intuitive analogues of the guiding principle behind SVMs, and aim to clearly separate the scores for rare versus dominant classes. Despite their success, such techniques are not without limitation. For example, when applied to neural models, they do not explicitly control the distribution of the learned embeddings themselves. This can be potentially sub-optimal, since embeddings for tail classes may be diffuse, as has been empirically observed [Zhang et al., 2017, Yin et al., 2019, Liu et al., 2019, Zhong et al., 2019, Ye et al., 2020, Samuel and Chechik, 2021, Wang et al., 2021b].

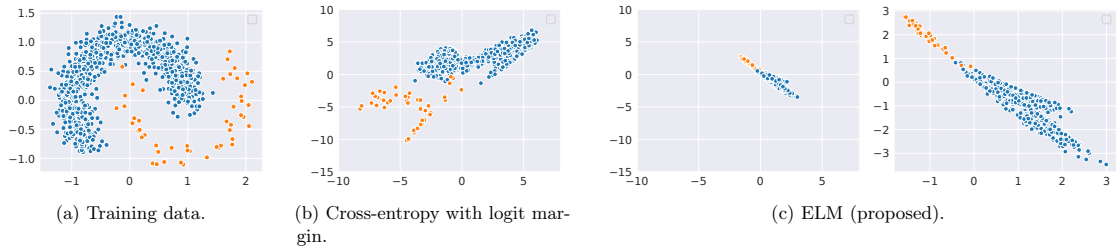


Figure 1: Illustration of embeddings produced from a three-layer ReLU network trained on an imbalanced variant of the two-moon problem. The embeddings learned by our proposed ELM regulariser are more compact than those from cross-entropy with logit margins. In particular, embeddings from the rare class (orange) are pulled more tightly together. See §2.3 for details.

In this paper, we present ELM, a framework that enforces both *Embedding and Logit Margins*. In a nutshell, ELM enforces margins in logit space, and regularize the distribution of embeddings. This connects losses for long-tail learning to proposals in the literature on metric learning [Weinberger and Saul, 2009], and contrastive learning [Khosla et al., 2020]. Theoretically, we show how ELM encourages a better approximation to the Bayes solution, by ensuring that class-conditionals are more Gaussian. Empirically, ELM is shown to perform well, and results in tighter embeddings (cf. Figure 1). In sum, our contributions are:

- (i) we propose ELM (4), a technique that enforces both embedding and logit margins for long-tail learning, leveraging insights from metric [Weinberger and Saul, 2009] and representation learning [Wen et al., 2016];
- (ii) we establish the benefits of enforcing embedding and logit margins, by showing that ELM encourages a better approximation to the Bayes-optimal classifier (§4); and,
- (iii) we present experiments on synthetic and real-world datasets that confirm the value of ELM against existing methods (§5), and in particular demonstrate the import of enforcing margins in both logit and embedding space.

2 Background and Notation

2.1 Multi-Class Classification

Let \mathcal{X} be the domain of input instances, and $\mathcal{Y} = [L] \doteq \{1, \dots, L\}$ be the domain of class labels. Given a training sample $S \doteq \{(x_i, y_i)\}_{i=1}^N \stackrel{\text{i.i.d.}}{\sim} \mathbb{P}^N$ where \mathbb{P} is a joint distribution defined on $\mathcal{X} \times \mathcal{Y}$, the goal of the multi-class classification problem is to learn a *scorer* $f: \mathcal{X} \rightarrow \mathbb{R}^L$ with $f(x) = (f_1(x), \dots, f_L(x))^\top$ so as to minimize the expected loss $\ell: \mathcal{Y} \times \mathbb{R}^L \rightarrow \mathbb{R}_+$. That is, one solves the following optimization problem:

$$\min_{f \in \mathcal{F}} R(f) \doteq \mathbb{E}_{(x,y) \sim \mathbb{P}} [\ell(y, f(x))], \quad (1)$$

where \mathcal{F} is a class of models for the scorer. For the zero-one loss $\ell_{01}(y, f(x)) \doteq \mathbb{I}[y \in \arg \max_{y' \in \mathcal{Y}} f_{y'}(x)]$, (1) coincides with the notion of misclassification error. Since ℓ_{01} is not differentiable, a commonly used surrogate loss is the softmax cross entropy $\ell_{\text{CE}}(y, f(x)) \doteq -\log \left[\frac{e^{f_y}}{\sum_{y' \in \mathcal{Y}} e^{f_{y'}}} \right] = \log \left[1 + \sum_{y' \neq y} e^{f_{y'}(x) - f_y(x)} \right]$. Since f is an argument to the softmax function, $f_1(x), \dots, f_L(x)$ are also known as the logits for x .

2.2 Long-Tail Learning

Practical classification problems often possess a skewed label distribution $\mathbb{P}(y)$. This problem of learning under *class imbalance* is a classical area of study [Kubat et al., 1997, Chawla et al., 2002, He and Garcia, 2009], which has received renewed interest in the context of neural models in the area of *long-tail learning* [Van Horn and Perona, 2017, Buda et al., 2017, Liu et al., 2019, Johnson and Khoshgoftaar, 2019]. The core challenge in such settings is ensuring that rare labels are not systematically misclassified, owing to their limited representation in the training data.

Formally, this is typically encapsulated as the goal of minimising the *balanced error*, which posits a uniform label distribution $\mathbb{P}(y)$ for evaluation:

$$\min_{f \in \mathcal{F}} R_{\text{bal}}(f) \doteq \frac{1}{L} \sum_{y \in [L]} \mathbb{E}_{x|y} [\ell(y, f(x))]. \quad (2)$$

Most successful approaches follow one of three strategies:

- (i) modifying the training data to make it more balanced (e.g., by up- or down-sampling different labels [Kubat and Matwin, 1997, Chawla et al., 2002, Wallace et al., 2011, Mikolov et al., 2013, Xue and Hall, 2015, Mahajan et al., 2018, Yin et al., 2019, Zhang et al., 2019]),
- (ii) modifying the classification rule to ensure greater representation of rare classes (e.g., applying per-class thresholds [Fawcett and Provost, 1996, Provost, 2000, Maloof, 2003, King and Zeng, 2001, Collell et al., 2016, Kang et al., 2020, Zhang et al., 2021]), and
- (iii) modifying the loss function to penalise errors on rare labels more strongly (e.g., by introducing appropriate asymmetry [Zhang et al., 2017, Cui et al., 2019, Cao et al., 2019, Tan et al., 2020, Jamal et al., 2020, Ren et al., 2020, Wu et al., 2020, Menon et al., 2021, Deng et al., 2021, Kini et al., 2021, Wang et al., 2021a]).

The above is not exhaustive, and other strategies have also been pursued [Yang and Xu, 2020, Sahoo et al., 2020, Liu et al., 2019, 2020, Chu et al., 2020, Tang et al., 2020, Samuel and Chechik, 2021, Ye et al., 2021]. Amongst loss modification techniques, a popular strategy involves augmenting the softmax cross-entropy with *logit margins*. Specifically, these involve an instantiation of the loss

$$\ell_{\text{mar}}(y, f(x)) \doteq \log \left[1 + \sum_{y' \neq y} e^{\Delta_{yy'} + f_{y'}(x) - f_y(x)} \right], \quad (3)$$

where $\Delta_{yy'}$ is some set of margins between labels y and y' . Examples of such Δ include $\Delta_{yy'} = \frac{1}{\mathbb{P}(y)^{1/4}}$ [Cao et al., 2019], $\Delta_{yy'} = \mathbb{P}(y')$ [Tan et al., 2020], and $\Delta_{yy'} = \log \frac{\mathbb{P}(y')}{\mathbb{P}(y)}$ [Ren et al., 2020, Menon et al., 2021, Wang et al., 2021a]. Intuitively, such a loss can be seen as a soft approximation to $\max_{y' \neq y} [\Delta_{yy'} + f_{y'}(x) - f_y(x)]_+$, where $[a]_+ \doteq \max(0, a)$, and thus encourages a sufficiently large gap between the logits for y and y' . By ensuring that $\Delta_{yy'}$ is large for rare “positive” labels y and/or dominant “negative” labels y' , one mitigates confusing a rare label for a dominant one. In the sequel, we shall primarily be interested in the choice $\Delta_{yy'} = \log \frac{\mathbb{P}(y')}{\mathbb{P}(y)}$, which possesses good empirical performance compared to alternatives [Ren et al., 2020, Menon et al., 2021, Wang et al., 2021a].

2.3 The Limits of Logit Margins

While logit margins have enjoyed considerable success, they alone may not be enough to guarantee accurate predictions for tail samples. Consider a synthetic setup, where we have 2D data with binary labels {Head, Tail}, following a similar setup to the “two moons” distribution [Zhou et al., 2003]. We set $\mathbb{P}(y = \text{Tail}) = 5\%$, so that the label distribution is imbalanced. To learn a nonlinear classifier, we use a three layer feedforward network with ReLU activation, with {16, 8, 2} hidden units respectively.

The use of two hidden units for the pre-output layer facilitates ready visualization. Figure 1 illustrates the learned embeddings under minimisation of the cross-entropy with the logit-adjusted

margin (3), which achieves near perfect test accuracy. Despite their good performance, we see that the learned embeddings are diffuse. By contrast, the embeddings for each class become relatively more compact under the proposed ELM regulariser, which we now detail.

3 ELM: Embedding and Logit Margins

We now present ELM, a technique that augments margins in both logit and embedding space.

3.1 Formulation

Consider a scorer $f_y(x) = w_y^\top \Phi(x) + b_y$, where $w_y \in \mathbb{R}^K$ are the classification weights for label y , $b_y \in \mathbb{R}$ is a bias term, and $\Phi(x) \in \mathbb{R}^K$ the learned embeddings for instance x . The ELM objective is:

$$\min_{w, \Phi} \frac{1}{N} \sum_{(x, y) \in S} [\ell_{\text{mar}}(y, f(x)) + \lambda \cdot \Omega_{\text{pull}}(x, y)], \quad (4)$$

where ℓ_{mar} is per (3), and $S \doteq \{(x_i, y_i)\}_{i=1}^N \stackrel{\text{i.i.d.}}{\sim} \mathbb{P}^N$ is a training sample from the joint distribution \mathbb{P} . Furthermore, $\lambda \geq 0$ controls the trade-off between logit margin (promoted by ℓ_{mar}) and embedding margin (encouraged by Ω_{pull}). Inspired by objectives in metric learning [Weinberger and Saul, 2009], we shall consider

$$\Omega_{\text{pull}}(x, y) \doteq \log \left[1 + \sum_{x^+ \in S_y \setminus \{x\}} e^{\|\Phi(x) - \Phi(x^+)\|_2^2 - \alpha_y} \right],$$

where S_y denotes the training samples with label y . Intuitively, Ω_{pull} acts to “pull” together embeddings from the same class. Further, parameters $\{\alpha_y\}_{y \in [L]}$ serve as margins that control the desired slack in enforcing this consideration. Intuitively, we seek to ensure that rare classes are pulled tightly together (i.e., small α_y). The pull regulariser Ω_{pull} can be seen as a differentiable relaxation of

$$\tilde{\Omega}_{\text{pull}}(x, y) \doteq \max_{x^+ \in S_y \setminus \{x\}} [\|\Phi(x) - \Phi(x^+)\|_2^2 - \alpha_y]_+,$$

which pulls together embeddings of the same class y so that, on average, each pair is no more than α_y away. Observe that $\tilde{\Omega}_{\text{pull}}(x, y) < \Omega_{\text{pull}}(x, y)$.

With more uncertainty associated with rare classes, it is reasonable to pull their embeddings together more strongly than those from frequent classes. This implicitly ensures that embeddings of rare classes are well-separated from other classes and helps accommodate embeddings of unobserved instances during test time, which may have high variance. In line with these, we thus propose setting $\alpha_y \propto \mathbb{P}(y)^a$ where $a > 0$. In the sequel, we shall focus on $a = 1$ or $a = \frac{1}{2}$. A similar consideration was made by Samuel and Chechik [Samuel and Chechik 2021], as shall be detailed in §3.2.

3.2 Connection to Existing Work

The core elements of the ELM objective (4) are not without precedent. For example, the idea of regularising embeddings has been widely explored in the area of contrastive learning [Wu et al., 2018, van den Oord et al., 2018, Khosla et al., 2020]. Similarly, the idea of having the pull term underpins Fisher linear discriminant analysis [FISHER, 1936]. However, the key to ELM’s success in long-tailed problems is enforcing *margins* in both the logit and embedding space, and having these margins be sensitive to the label distribution $\mathbb{P}(y)$. We now detail the relevant strands of prior work, and delineate the key differences to ELM. (See Table 1.)

Table 1: Summary of approaches to learning with logit and embedding margins. Here, “long tail” refers to whether or not the method explicitly accounts for skew in the label distribution; “logit loss” refers to whether or not the method explicitly learns logits for classification, as opposed to relying on a k -NN classifier; and “embedding loss” refers to whether or not the method explicitly regularises the embeddings in some way, as opposed to purely operating on logits. In long-tail settings, enforcing a logit margin is essential to ensure consistency for the balanced error, while enforcing an embedding margin is essential to ensure compactness of the embeddings on tail classes. Entries marked “—” are not applicable.

Method	Long tail?	Logit loss?	Logit margin?	Embedding loss?	Embedding margin?
Contrastive loss [Sun et al., 2014, Wu et al., 2018, van den Oord et al., 2018, He et al., 2019, Chen et al., 2020]	—	—	—	✓	×
Supervised contrastive loss [Khosla et al., 2020, Chuang et al., 2020]	×	×	—	✓	×
Triplet loss [Weinberger and Saul, 2009, Hadsell et al., 2006, Schroff et al., 2015, Sohn, 2016]	×	×	—	✓	✓
Spreadout [Zhang et al., 2017]	×	✓	×	✓	×
Center loss [Wen et al., 2016]	×	✓	×	✓	×
Hybrid contrastive learning [Liu and Abbeel, 2020]	×	✓	×	✓	×
Softmax with margin [Cao et al., 2019, Tan et al., 2020, Ren et al., 2020, Menon et al., 2013, Wang et al., 2021a]	✓	✓	✓	×	—
Range loss [Zhang et al., 2017]	✓	✓	×	✓	✓
DRO-LT [Samuel and Chechik, 2021]	✓	✓	×	✓	✓
Ours	✓	✓	✓	✓	✓

Contrastive learning Contrastive learning [Wu et al., 2018, Sun et al., 2014, van den Oord et al., 2018, He et al., 2019, Chen et al., 2020] techniques seek to learn good representations $\Phi: \mathcal{X} \rightarrow \mathbb{R}^K$ by aligning similar instances (e.g., a sample and its perturbation), and pushing apart dissimilar instances (e.g., pairs of random samples). This may be achieved by minimising $\Omega_{\text{con}}(x) \doteq$

$$\mathbb{E}_{x^+, \mathcal{N}(x)} \log \left[1 + \sum_{x^- \in \mathcal{N}(x)} e^{\Phi(x)^{\top} \Phi(x^-) - \Phi(x)^{\top} \Phi(x^+)} \right],$$

where x^+ is a “positive” sample for x , and $\mathcal{N}(x)$ comprises contrasting “negative” samples for x . In standard contrastive learning, there is no explicit supervision, and so $\mathcal{N}(x)$ may be taken to be randomly sampled inputs. In supervised contrastive learning [Khosla et al., 2020, Chuang et al., 2020], it is assumed that label information is present, and $\mathcal{N}(x)$ comprises samples with a different label than x, x^+ . Such techniques do *not* involve a logit margin, and are not adapted to long-tail settings.

Objectives based on the triplet loss take a similar form [Weinberger and Saul, 2009, Hadsell et al., 2006, Schroff et al., 2015, Sohn, 2016], with the contrasting set $\mathcal{N}(x)$ comprising one or more negative samples, typically chosen based on some form of negative mining. Most such objectives enforce an explicit margin, i.e., for $\gamma > 0$,

$$\Omega_{\text{trip}}(x) \doteq \mathbb{E}_{x^+, x^-} [\gamma + \Phi(x)^{\top} \Phi(x^-) - \Phi(x)^{\top} \Phi(x^+)]_+.$$

Here, γ is constant across all samples, and is thus not attuned to skewed label distributions.

Classification-contrastive hybrids Recently, Samuel and Chechik [2021] proposed DRO-LT, which adds the regulariser $\Omega_{\text{dro}}(x, y) \doteq$

$$\log \left[\sum_{(x', y') \in S} e^{-\|\Phi(x') - \mu_y\|_2^2 + \|\Phi(x) - \mu_y\|_2^2 + \epsilon_y \cdot \mathbb{I}(y' \neq y)} \right], \quad (5)$$

where S is the set of all instance-label pairs, $\epsilon_y \propto 1/\sqrt{\mathbb{P}(y)}$, and μ_y is the centroid in the embedding space of all samples in class y . Wang et al. [2021b] proposed a similar loss with $\epsilon_y = 0$. Like our ELM method, DRO-LT explicitly seeks to improve the quality of learned embeddings for tail classes. However, there are important distinctions:

- (i) DRO-LT is somewhat pessimistic, in that it pushes away the embedding for a sample (x, y) to *all* other samples (x^+, y') , regardless of whether $y' = y$. (Samples with $y' \neq y$ are however subject to a margin of $\epsilon_y > 0$.) As demonstrated in Figure 4, this can cause the embeddings for a given class to be *more* spread out compared to ERM. By contrast, we only separate samples from different classes (by the logit-adjusted cross-entropy term), and pull together samples from the same class.
- (ii) we give a unified treatment of margins in both logit and embedding space. In particular, we justify our approach in terms of approximation to the Bayes solution (§4).

Liu and Abbeel [2020] proposed to combine the softmax cross-entropy with a contrastive-like term:

$$\Omega(x, y) \doteq \log \left[1 + \sum_{x^- \in \mathcal{N}(x)} e^{f_y(x^-) - f_y(x)} \right].$$

A similar objective was also considered in Veit and Wilber [2020]. Compared to our approach, there are two key distinctions. First, there is no margin enforced in either term. Second, the contrastive term operates in logit space, and thus changes the target function in a non-trivial manner; in a long-tail setting, this would erase the consistency guarantees for the balanced error [Menon et al., 2021].

Improved embeddings for tail classes For long-tail settings, some works have considered means of improving embeddings for tail classes. For example, in Zhang et al. [2017], it was proposed to minimise

$$\Omega_{\text{range}}(x) \doteq \max_{y \neq y'} [\gamma - \|\mu_y - \mu_{y'}\|_2^2]_+,$$

so that different classes’ centroids are pushed apart. There are three important points worth mentioning. First, it is based on a hard max, which allows for limited gradient propagation. Second, the margin γ is the same for all labels, and is not attuned to tail classes. Third, this does not consider logit margins, which we demonstrate can lead to suboptimal decision boundaries.

Yin et al. [2019], Liu et al. [2019] proposed to transfer information from dominant to rare class embeddings directly. This is an interesting yet orthogonal consideration to improving the spread and separation of tail embeddings; its fusion with the ideas of the present paper would be of interest in future work. For discussion of additional related work, see Appendix D.

4 Analysis: Why Does ELM help?

At its core, ELM enforces logit *and* embedding margins. Both of these help improve performance, as we now argue.

4.1 Why Do Margins Help?

The case for logit margins has already been made in prior work [Cao et al., 2019, Tan et al., 2020, Ren et al., 2020, Menon et al., 2021, Wang et al., 2021a], but is worth succinctly recapitulating. There are two key arguments: first, for generic supervised learning problems, margin bounds [Bartlett et al., 1998, Koltchinskii and Panchenko, 2002, Bartlett et al., 2017] establish that large margins imply good generalisation. Second, for long-tail problems in particular, excluding logit margins would implicitly seek to model $\mathbb{P}(y | x)$; absent further correction, this solution will be suboptimal for the balanced error [Menon et al., 2013, Collell et al., 2016, Ren et al., 2020, Menon et al., 2021].

Embedding margins are useful if we want to use a k -nearest neighbour classifier as a post-hoc training procedure. Such post-hoc training procedures have proven successful in long-tail settings [Kang et al., 2020]. More fundamentally, however, one may justify the regularisation of these embeddings from the perspective of approximating the Bayes-optimal decision boundary, as we now see.

4.2 ELM and the Bayes-Optimal Classifier

We now quantify the value of the pull term in ELM (4).

Proposition 1. *Let $\bar{\Omega}_{\text{pull}}(y) \doteq \frac{1}{|S_y|} \sum_{x \in S_y} \Omega_{\text{pull}}(x, y)$ and $\Phi(x) \doteq (\Phi_1(x), \dots, \Phi_K(x))^\top$. Then,*

$$\frac{2|S_y|}{|S_y| - 1} \cdot \sum_{j=1}^K \hat{\mathbb{V}}[\Phi_j(x) | y] - \alpha_y + \log(|S_y| - 1) \leq \bar{\Omega}_{\text{pull}}(y).$$

Here, $\hat{\mathbb{V}}[\cdot | y]$ is the empirical conditional variance of class y . Proposition 1 (proof in Appendix C.1) states that minimizing the class-wise average of the pulling objective Ω_{pull} will also minimize the sum of class-conditional variances (in the embedding space) of all dimensions; i.e., the pulling objective encourages a small intra-class variance. As shall be seen later in Proposition 2, reduction of class-conditional variances directly translates to better generalisation. Expanding the result stated in Proposition 1, we have

$$\begin{aligned} & \frac{1}{|S_y|} \sum_{x \in S_y} \Omega_{\text{pull}}(x, y) \\ & \geq \frac{2|S_y|}{|S_y| - 1} \sum_{x \in S_y} \|\Phi(x) - \mu_y\|^2 - \alpha_y + \log(|S_y| - 1), \end{aligned}$$

where μ_y is the centroid of all embeddings in class y . The first term on the right hand side is exactly the regulariser in the center loss [Wen et al., 2016]. This may be interpreted as encouraging a more Gaussian distribution for the embeddings: indeed,

$$\begin{aligned} & \sum_{x \in S_y} \|\Phi(x) - \mu_y\|_2^2 \\ & = \sum_{x \in S_y} -\log \mathbf{N}(\Phi(x); \mu_y, \sigma_y^2 I) + \text{constant}, \end{aligned}$$

i.e., it is the log-likelihood under an isotropic Gaussian model for $\mathbf{Z} | \mathbf{Y} = y$, where we define the random vector $\mathbf{Z} \doteq \Phi(\mathbf{X})$ and $\mathbf{X} \sim \mathbb{P}(x)$. The value of such a model is that *it justifies the use of a softmax distribution for the final layer*. In particular, when $\mathbf{Z} | \mathbf{Y} = y \sim \mathbf{N}(\mu_y, \sigma_y^2 I)$,

$$\begin{aligned} \mathbb{P}(y | z) & \propto \mathbb{P}(z | y) \cdot \mathbb{P}(y) \\ & \propto \exp\left(\Phi(x)^\top \frac{\mu_y}{\sigma_y^2} - \frac{\|\mu_y\|_2^2}{2\sigma_y^2} + \log \mathbb{P}(y)\right), \end{aligned}$$

where $z = \Phi(x)$ denotes a realization of \mathbf{Z} . Thus, under a Gaussian distribution for embeddings, we may perfectly express $\mathbb{P}(y | x)$ as an affine function of $\Phi(x)$, composed with a softmax link function.

4.3 Generalisation Bound

We now present a generalisation bound of the logit-adjusted cross-entropy loss (3) in Proposition 2. We consider the binary case where $y \in \{-1, +1\}$. In this case, it is sufficient to consider a real-valued scorer $f(x) \doteq w^\top \Phi(x) + b \in \mathbb{R}$ that computes the logit for class +1. Accordingly, the logit-adjusted cross-entropy loss in (3) can be written as $\ell_{\log}(y, f(x) + \Delta_y) := \log [1 + e^{-y(f(x) + \Delta_y)}]$.

Proposition 2. *Let $\Delta_y \in \mathbb{R}$, and $\ell_{\log}(y, f(x) + \Delta_y) := \log [1 + e^{-y(f(x) + \Delta_y)}]$. Suppose $y \in \{-1, 1\}$, and $\sup_{x \in \mathcal{X}, y \in \{-1, 1\}} \ell_{\log}(y, f(x) + \Delta_y) \leq B$ for some $B \in (0, \infty)$. Then, given $f(x) \doteq w^\top \Phi(x) + b \in \mathbb{R}$, with probability at least $1 - \delta$,*

$$\begin{aligned} & \mathbb{E}_{(x,y) \sim \mathbb{P}_{xy}} \ell_{\log}(y, f(x) + \Delta_y) \\ & \leq \frac{7B \ln 2/\delta}{3} \sum_{y \in \{-1, 1\}} \frac{\mathbb{P}(y)}{|S_y| - 1} + \sum_{y \in \{-1, 1\}} \frac{\mathbb{P}(y)}{|S_y|} \sum_{x \in S_y} \ell_{\log}(y, f(x) + \Delta_y) \\ & \quad + \|w\| \sqrt{\ln \frac{2}{\delta} \sum_{y \in \{-1, 1\}} \frac{\mathbb{P}(y)}{|S_y|} [\bar{\Omega}_{\text{pull}}(y) + \alpha_y]}, \end{aligned}$$

where $\bar{\Omega}_{\text{pull}}(y) \doteq \frac{1}{|S_y|} \sum_{x \in S_y} \Omega_{\text{pull}}(x, y)$.

Proposition 2 suggests that the generalisation gap of classifiers trained with the softmax cross-entropy with logit margins (see (3)) can be expressed as a function of the proposed pull term Ω_{pull} . This justifies its use in the ELM (see (4)) as encouraging better generalisation. The improvement from adding a pull term to the logit-adjusted loss results in a larger gap between the per-class logits, and a more compact per-class distribution of embeddings, as shall be seen in §5.

Note that the difference between $\frac{1}{N} \sum_{(x,y) \in S} \ell_{\log}(y, f(x) + \Delta_y)$ and $\sum_{y \in \{-1, 1\}} \frac{\mathbb{P}(y)}{|S_y|} \sum_{x \in S_y} \ell_{\log}(y, f(x) + \Delta_y)$ vanishes as $N \rightarrow \infty$. The former thus approximates the empirical error of the logit-adjusted loss ℓ_{mar} , and aligns with our formulation in (4). Further note that while the generalisation error on the left-hand side of the bound is with respect to the joint distribution (which depends on the skewed label distribution $\mathbb{P}(y)$), it is consistent for minimising the balanced error where the label distribution is uniform when $\Delta_y = \log \frac{\mathbb{P}(y=+1)}{\mathbb{P}(y=-1)}$ [Menon et al., 2021].

5 Experiments on Long-tail Benchmarks

We present results confirming that ELM performs well on benchmarks for long-tail learning.

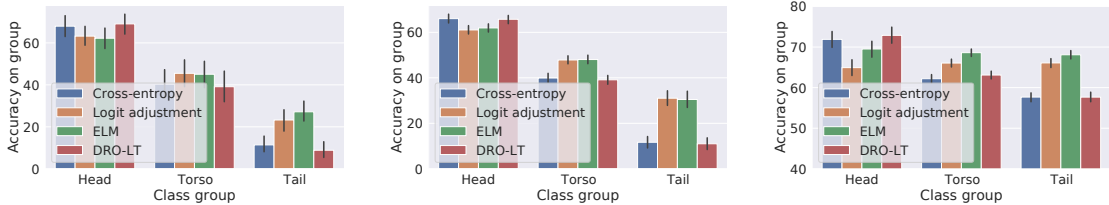
Datasets We present results on image classification benchmarks for long-tail learning: CIFAR10-LT, CIFAR100-LT, ImageNet-LT and iNaturalist 2018. Each of these datasets has a skewed training set, and balanced test set. The long-tailed (“LT”) CIFAR datasets are constructed by downsampling labels from the original CIFAR train sets, following the EXP profile of Cui et al. [2019], Cao et al. [2019] with imbalance ratio $\rho = \max_y \mathbb{P}(y) / \min_y \mathbb{P}(y) = 100$. The long-tailed ImageNet dataset is as constructed in Liu et al. [2019], and iNaturalist as per Van Horn and Perona [2017].

Models We employ a CIFAR-ResNet-32 for the CIFAR datasets, and a ResNet-50 for ImageNet and iNaturalist. See Appendix A for details on training hyper-parameters, which follow Menon et al. [2021].

Baselines We compare the proposed ELM method (4) in terms of *balanced* test set accuracy against several baselines: (i) cross-entropy (**CE**) minimisation; (ii) the class-balanced (**CB Focal**) loss of Cui et al. [2019], which applies asymmetric weights on the per-class losses; (iii) **LDAM+DRW** [Cao et al., 2019], which enforces a logit margin; (iv) the logit adjustment (**LogAdj**) loss [Ren et al., 2020,

Table 2: Test set accuracy (averaged over 3 trials) on real-world datasets. Here, *, ‡, †, ◊ are numbers for “ τ -normalised” from Kang et al. [2020, Table 3, 7]; “Class-Balanced” from Cui et al. [2019, Table 2, 3]; “LDAM + DRW” from Cao et al. [2019, Table 2, 3]; “DRO-LT” from Samuel and Chechik [2021, Table 1, 2]. The faded cells denote “multi-stage” methods requiring training multiple models. The others, including our proposed ELM, perform training in one-stage. Our goal is to understand the performance we can get from a one-stage training procedure.

Method	CIFAR10-LT	CIFAR100-LT	ImageNet-LT	iNaturalist
Cross-entropy (CE)	72.84	38.36	45.20	61.34
CB Focal [Cui et al., 2019]	74.57‡	39.60‡	46.79	64.16‡
LDAM + DRW [Cao et al., 2019]	77.03†	42.04†	50.15	68.00†
LogAdj [Ren et al., 2020, Menon et al., 2021, Wang et al., 2021a]	77.67	43.89	50.37	66.36
CE + DRO-LT (one-stage) [Samuel and Chechik, 2021]	72.70	41.98	45.70	62.05
CE + weight normalisation (multi-stage) [Kang et al., 2020]	78.50	41.34	50.63	65.60*
CE + DRO-LT (multi-stage) [Samuel and Chechik, 2021]	80.50	46.92◊	53.00◊	69.70◊
ELM (proposed, one-stage)	77.95	45.77	50.60	68.71



(a) CIFAR100-LT (100 classes). (b) Imagenet-LT (1000 classes). (c) iNaturalist (8142 classes).

Figure 2: Breakdown of per-label accuracies, where labels are bucketed into groups based on their frequency. Compared to enforcing logit margins, additionally enforcing embedding margins are seen to help as ELM improves upon LogAdj on the Torso and Tail groups.

Menon et al., 2021, Wang et al., 2021a], which enforces a logit margin per (3); (v) **DRO-LT** [Samuel and Chechik, 2021], which enforces an embedding margin $\epsilon_y \propto \mathbb{P}(y)^{-1/2}$. For ELM, we set the logit margin $\Delta_{yy'} = \log \frac{\mathbb{P}(y')}{\mathbb{P}(y)}$, following the **LogAdj** loss; thus, ELM imposes additional regularisers over this method. We detail the choice of α_y in the Appendix.

One- versus multi-stage methods We remark here that DRO-LT is a “multi-stage” method, as it requires first obtaining centroid estimates μ_y from CE training; training using these, plus the DRO-LT regulariser (5); and finally training a balanced classifier on the resulting embeddings. By contrast, all other baselines — and the proposed ELM — are “one-stage” methods. Thus, for an equitable comparison, we consider a “one-stage” version of DRO-LT, which does not have a separate estimation of μ_y , nor retraining of a linear model on the learned embeddings. For completeness, we additionally quote the results of multi-stage DRO-LT from Samuel and Chechik [2021]. As another multi-stage baseline, we report the results of post-hoc weight normalisation [Kang et al., 2020] on the CE solution.

An important goal of our experiments is to understand the performance (balanced accuracy) we can get from training in one stage. This helps understand losses for long-tailed learning without being occluded by benefits gained from the more generally applicable augmented procedures such as balanced sampling, and fine-tuning the classifier layer.

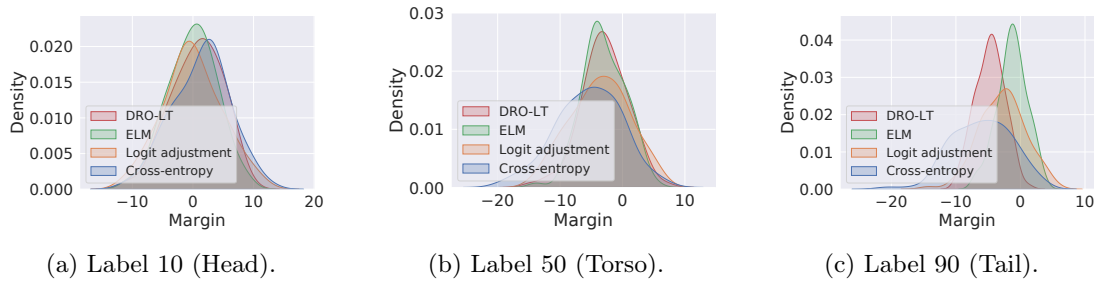


Figure 3: Margin plots on CIFAR100-LT. For a given label y , we plot the distribution of the margins $\gamma(x, y) \doteq f_y(x) - \max_{y' \neq y} f_{y'}(x)$ for instances x with label y . ELM is seen to consistently reduce the variance of the margin distribution, while also shifting it favourably over CE on the Tail label.

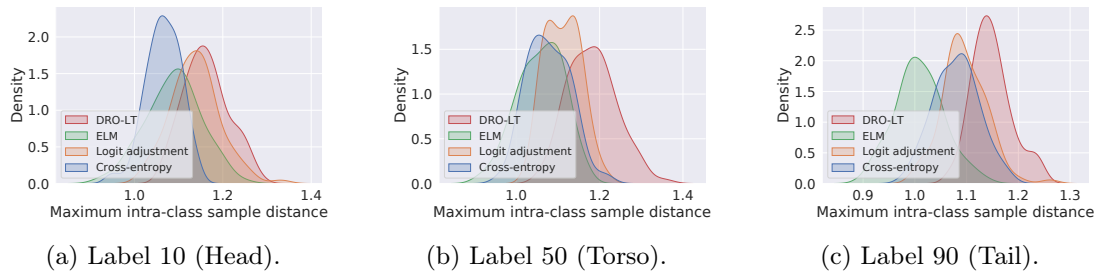


Figure 4: Maximum intra-class distances on CIFAR100-LT. For a given label y , we plot the distribution of the maximum intra-class distances $d_{\max}(x) \doteq \max_{x^+ \in S_y} \|\Phi(x) - \Phi(x^+)\|_2$ for instances x with label y ; distances are normalised by the maximal embedding norm $\max_{x \in S} \|\Phi(x)\|_2$. DRO-LT is seen to increase these distances slightly, owing to contrasting samples within the same class.

Results and analysis Table 2 presents the results on all datasets. We make some key observations. *Logit and embedding margins help.* In keeping with prior work, approaches that enforce a logit margin, e.g., LDAM [Cao et al., 2019], and LogAdj [Ren et al., 2020, Menon et al., 2021, Wang et al., 2021a], perform significantly better than CE. Similarly, one-stage CE + DRO-LT, which enforces an embedding margin, consistently improves over CE.

Compared to these techniques, combining both logit and embedding margins yields improvements, as shown by the performance of ELM, intuitively owing to it encouraging pulling together of similar embeddings. Interestingly, even when compared to a multi-stage version of DRO-LT, the performance of our one-stage ELM remains favourable, with only a small difference across all datasets.

Breakdown of performance. The above illustrates the ELM can improve the overall tradeoff between rare and dominant labels. For a more fine-grained understanding, following Kang et al. [2020], we break down the labels into three groups, termed “Head” (labels with ≥ 100 training samples), “Torso” ($[20, 100)$ samples), and “Tail” (< 20 samples). Figure 2 reveals that, per Menon et al. [2021], LogAdj achieves gains on both the Torso and Tail groups, at the mild expense of performance on the Head group. Further adding an embedding margin via ELM yields gains on the Torso and Tail groups. Interestingly, on the challenging iNaturalist data, there are gains on the Head group as well.

Analysis of logit margins. We analyse the distribution of logit margins $\gamma(x, y) \doteq f_y(x) - \max_{y' \neq y} f_{y'}(x)$ on CIFAR100-LT. We pick three labels from the Head, Torso, and Tail slices, and compare the margin distributions for the cross-entropy loss (CE), the logit adjustment (LogAdj) loss, the proposed ELM, and DRO-LT. Figure 3 visualises these margin distributions. As expected, logit adjustment tends to trade off performance on dominant classes, while significantly increasing margins on rare classes.

Interestingly, from Figure 3, ELM strongly controls the margin distribution, which becomes less

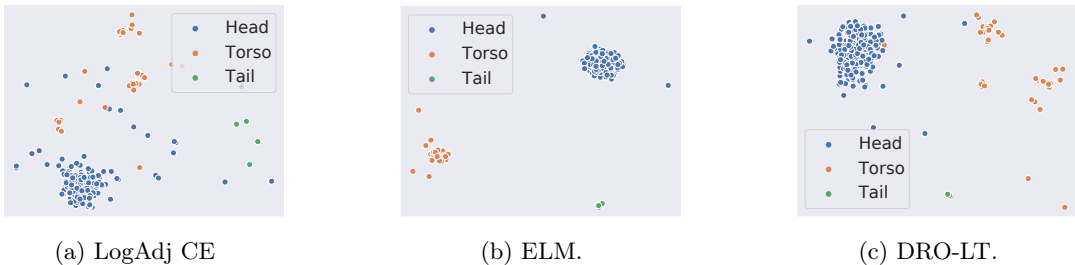


Figure 5: Training set embedding visualisations on CIFAR100-LT via tSNE. Shown are a sample of classes that have ≥ 100 associated samples (“Head”), $[20, 100)$ samples (“Torso”), and < 20 samples (“Tail”) in the training set. ELM produces more compact embeddings.

variable. Further, on the tail label, we see that ELM significantly shifts the mode of the margins over cross-entropy and LogAdj. As such logit margins directly control generalisation performance [Bartlett et al., 1998, 2017], this lends further credence to ELM improving classification performance as also suggested by Proposition 2.

Analysis of embeddings. We conduct a similar analysis on the distances between the learned embeddings. For instances x with label y , Figure 4 visualises the maximum intra-class distances $d_{\max}(x) = \max_{x^+ \in S_y} \|\Phi(x) - \Phi(x^+)\|_2$. The distances are normalised by the maximal embedding norm $\max_{x \in S} \|\Phi(x)\|_2$. We observe that DRO-LT increases the *intra*-class distances slightly compared to CE, owing to contrasting samples within the same class. By contrast, the pull part of ELM ensures that these distances remain small, thus encouraging tighter clusters, especially for tail classes.

To visually inspect the learned embeddings, we create 2D tSNE [van der Maaten and Hinton, 2008] visualisations of the embeddings learned by LogAdj, ELM, and DRO-LT. Figure 5 illustrates these embeddings for a sample of classes from the previously created Head, Torso and Tail buckets. ELM is seen to produce more compact and separated embeddings compared to logit-adjusted cross-entropy minimisation and DRO-LT. For additional experiments and ablations, we refer the reader to the Appendix.

6 Discussion and Future Work

The ELM method presents a unified approach to enforce margins in logit space, and regularise the distribution of embeddings. Our argument for the value of such regularisation is instructive, and such regularisation implies better generalisation as shown in Proposition 2. Yet a key question remains elusive: can we improve the performance of the tail group without trading off the performance of the head? The breakdown of per-group accuracies in Figure 2, especially on the challenging iNaturalist problem, offers some hope of this possibility. Exploring conditions under which this is possible would be a worthwhile direction for future work. More broadly, studying the efficacy of ELM in fairness settings with under-represented samples, to ensure it does not introduce unforeseen biases, is another important direction.

References

Peter Bartlett, Yoav Freund, Wee Sun Lee, and Robert E. Schapire. Boosting the margin: a new explanation for the effectiveness of voting methods. *The Annals of Statistics*, 26(5):1651 – 1686, 1998.

Peter L Bartlett, Dylan J Foster, and Matus J Telgarsky. Spectrally-normalized margin bounds for neural networks. In I. Guyon, U. V. Luxburg, S. Bengio, H. Wallach, R. Fergus, S. Vishwanathan,

- and R. Garnett, editors, *Advances in Neural Information Processing Systems*, volume 30. Curran Associates, Inc., 2017.
- Mateusz Buda, Atsuto Maki, and Maciej A. Mazurowski. A systematic study of the class imbalance problem in convolutional neural networks. *arXiv:1710.05381 [cs, stat]*, October 2017.
- Kaidi Cao, Colin Wei, Adrien Gaidon, Nikos Arechiga, and Tengyu Ma. Learning imbalanced datasets with label-distribution-aware margin loss. In *Advances in Neural Information Processing Systems*, 2019.
- Nitesh V. Chawla, Kevin W. Bowyer, Lawrence O. Hall, and W. Philip Kegelmeyer. SMOTE: Synthetic minority over-sampling technique. *Journal of Artificial Intelligence Research (JAIR)*, 16:321–357, 2002.
- Ting Chen, Simon Kornblith, Mohammad Norouzi, and Geoffrey Hinton. A simple framework for contrastive learning of visual representations. In Hal Daumé III and Aarti Singh, editors, *Proceedings of the 37th International Conference on Machine Learning*, volume 119 of *Proceedings of Machine Learning Research*, pages 1597–1607. PMLR, 13–18 Jul 2020.
- Peng Chu, Xiao Bian, Shaopeng Liu, and Haibin Ling. Feature space augmentation for long-tailed data. In Andrea Vedaldi, Horst Bischof, Thomas Brox, and Jan-Michael Frahm, editors, *Computer Vision – ECCV 2020*, pages 694–710, Cham, 2020. Springer International Publishing. ISBN 978-3-030-58526-6.
- Ching-Yao Chuang, Joshua Robinson, Yen-Chen Lin, Antonio Torralba, and Stefanie Jegelka. Debaised contrastive learning. In H. Larochelle, M. Ranzato, R. Hadsell, M. F. Balcan, and H. Lin, editors, *Advances in Neural Information Processing Systems*, volume 33, pages 8765–8775. Curran Associates, Inc., 2020.
- Guillem Collell, Drazen Prelec, and Kaustubh R. Patil. Reviving threshold-moving: a simple plug-in bagging ensemble for binary and multiclass imbalanced data. *CoRR*, abs/1606.08698, 2016.
- Yin Cui, Menglin Jia, Tsung-Yi Lin, Yang Song, and Serge Belongie. Class-balanced loss based on effective number of samples. In *CVPR*, 2019.
- Zongyong Deng, Hao Liu, Yaoxing Wang, Chenyang Wang, Zekuan Yu, and Xuehong Sun. PML: progressive margin loss for long-tailed age classification. *CoRR*, abs/2103.02140, 2021. URL <https://arxiv.org/abs/2103.02140>.
- Matthias Dorfer, Rainer Kelz, and Gerhard Widmer. Deep linear discriminant analysis. *arXiv preprint arXiv:1511.04707*, 2015.
- Tom Fawcett and Foster Provost. Combining data mining and machine learning for effective user profiling. In *Proceedings of the ACM SIGKDD International Conference on Knowledge Discovery and Data Mining (KDD)*, pages 8–13. AAAI Press, 1996.
- R. A. FISHER. The use of multiple measurements in taxonomic problems. *Annals of Eugenics*, 7 (2):179–188, 1936.
- Priya Goyal, Piotr Dollár, Ross B. Girshick, Pieter Noordhuis, Lukasz Wesolowski, Aapo Kyrola, Andrew Tulloch, Yangqing Jia, and Kaiming He. Accurate, large minibatch SGD: training imagenet in 1 hour. *CoRR*, abs/1706.02677, 2017. URL <http://arxiv.org/abs/1706.02677>.
- R. Hadsell, S. Chopra, and Y. LeCun. Dimensionality reduction by learning an invariant mapping. In *2006 IEEE Computer Society Conference on Computer Vision and Pattern Recognition (CVPR'06)*, volume 2, pages 1735–1742, 2006. doi: 10.1109/CVPR.2006.100.
- M. Hayat, S. Khan, S. Zamir, J. Shen, and L. Shao. Gaussian affinity for max-margin class imbalanced learning. In *2019 IEEE/CVF International Conference on Computer Vision (ICCV)*, pages 6468–6478, Los Alamitos, CA, USA, nov 2019. IEEE Computer Society.
- Haibo He and Edwardo A. Garcia. Learning from imbalanced data. *IEEE Transactions on Knowledge*

- and *Data Engineering*, 21(9):1263–1284, 2009.
- K. He, X. Zhang, S. Ren, and J. Sun. Deep residual learning for image recognition. In *2016 IEEE Conference on Computer Vision and Pattern Recognition (CVPR)*, 2016.
- Kaiming He, Haoqi Fan, Yuxin Wu, Saining Xie, and Ross Girshick. Momentum contrast for unsupervised visual representation learning. *arXiv preprint arXiv:1911.05722*, 2019.
- Muhammad Abdullah Jamal, Matthew Brown, Ming-Hsuan Yang, Liqiang Wang, and Boqing Gong. Rethinking class-balanced methods for long-tailed visual recognition from a domain adaptation perspective. In *Proceedings of the IEEE/CVF Conference on Computer Vision and Pattern Recognition (CVPR)*, June 2020.
- Justin Johnson and Taghi Khoshgoftaar. Survey on deep learning with class imbalance. *Journal of Big Data*, 6:27, 03 2019.
- Bingyi Kang, Saining Xie, Marcus Rohrbach, Zhicheng Yan, Albert Gordo, Jiashi Feng, and Yannis Kalantidis. Decoupling representation and classifier for long-tailed recognition. In *Eighth International Conference on Learning Representations (ICLR)*, 2020.
- Prannay Khosla, Piotr Teterwak, Chen Wang, Aaron Sarna, Yonglong Tian, Phillip Isola, Aaron Maschiot, Ce Liu, and Dilip Krishnan. Supervised contrastive learning. In H. Larochelle, M. Ranzato, R. Hadsell, M. F. Balcan, and H. Lin, editors, *Advances in Neural Information Processing Systems*, volume 33, pages 18661–18673. Curran Associates, Inc., 2020.
- Gary King and Langche Zeng. Logistic regression in rare events data. *Political Analysis*, 9(2): 137–163, 2001.
- Ganesh Ramachandra Kini, Orestis Paraskevas, Samet Oymak, and Christos Thrampoulidis. Label-imbalanced and group-sensitive classification under overparameterization. *CoRR*, abs/2103.01550, 2021. URL <https://arxiv.org/abs/2103.01550>.
- V. Koltchinskii and D. Panchenko. Empirical Margin Distributions and Bounding the Generalization Error of Combined Classifiers. *The Annals of Statistics*, 30(1):1 – 50, 2002.
- Walid Krichene, Nicolas Mayoraz, Steffen Rendle, Li Zhang, Xinyang Yi, Lichan Hong, Ed Chi, and John Anderson. Efficient training on very large corpora via gramian estimation. In *International Conference on Learning Representations*, 2019.
- Miroslav Kubat and Stan Matwin. Addressing the curse of imbalanced training sets: One-sided selection. In *Proceedings of the International Conference on Machine Learning (ICML)*, 1997.
- Miroslav Kubat, Robert Holte, and Stan Matwin. Learning when negative examples abound. In Maarten van Someren and Gerhard Widmer, editors, *Proceedings of the European Conference on Machine Learning (ECML)*, volume 1224 of *Lecture Notes in Computer Science*, pages 146–153. Springer Berlin Heidelberg, 1997. ISBN 978-3-540-62858-3.
- Hao Liu and Pieter Abbeel. Hybrid discriminative-generative training via contrastive learning. *CoRR*, abs/2007.09070, 2020. URL <https://arxiv.org/abs/2007.09070>.
- Jialun Liu, Yifan Sun, Chuchu Han, Zhaopeng Dou, and Wenhui Li. Deep representation learning on long-tailed data: A learnable embedding augmentation perspective. In *Proceedings of the IEEE/CVF Conference on Computer Vision and Pattern Recognition (CVPR)*, June 2020.
- Ziwei Liu, Zhongqi Miao, Xiaohang Zhan, Jiayun Wang, Boqing Gong, and Stella X. Yu. Large-scale long-tailed recognition in an open world. In *IEEE Conference on Computer Vision and Pattern Recognition, CVPR 2019, Long Beach, CA, USA, June 16-20, 2019*, pages 2537–2546. Computer Vision Foundation / IEEE, 2019.
- Dhruv Mahajan, Ross Girshick, Vignesh Ramanathan, Kaiming He, Manohar Paluri, Yixuan Li, Ashwin Bharambe, and Laurens van der Maaten. Exploring the limits of weakly supervised pretraining. In Vittorio Ferrari, Martial Hebert, Cristian Sminchisescu, and Yair Weiss, editors,

- Computer Vision – ECCV 2018*, pages 185–201, Cham, 2018. Springer International Publishing. ISBN 978-3-030-01216-8.
- Marcus A. Maloof. Learning when data sets are imbalanced and when costs are unequal and unknown. In *ICML 2003 Workshop on Learning from Imbalanced Datasets*, 2003.
- Andreas Maurer and Massimiliano Pontil. Empirical bernstein bounds and sample variance penalization. *arXiv preprint arXiv:0907.3740*, 2009.
- Aditya Krishna Menon, Harikrishna Narasimhan, Shivani Agarwal, and Sanjay Chawla. On the statistical consistency of algorithms for binary classification under class imbalance. In *Proceedings of the 30th International Conference on Machine Learning, ICML 2013, Atlanta, GA, USA, 16-21 June 2013*, pages 603–611, 2013.
- Aditya Krishna Menon, Sadeep Jayasumana, Ankit Singh Rawat, Himanshu Jain, Andreas Veit, and Sanjiv Kumar. Long-tail learning via logit adjustment. In *International Conference on Learning Representations*, 2021.
- Tomas Mikolov, Ilya Sutskever, Kai Chen, Greg Corrado, and Jeffrey Dean. Distributed representations of words and phrases and their compositionality. In *Proceedings of the 26th International Conference on Neural Information Processing Systems, NIPS’13*, pages 3111–3119, Red Hook, NY, USA, 2013. Curran Associates Inc.
- Foster Provost. Machine learning from imbalanced data sets 101. In *Proceedings of the AAAI-2000 Workshop on Imbalanced Data Sets*, 2000.
- Jiawei Ren, Cunjun Yu, shunan sheng, Xiao Ma, Haiyu Zhao, Shuai Yi, and hongsheng Li. Balanced meta-softmax for long-tailed visual recognition. In H. Larochelle, M. Ranzato, R. Hadsell, M. F. Balcan, and H. Lin, editors, *Advances in Neural Information Processing Systems*, volume 33, pages 4175–4186. Curran Associates, Inc., 2020.
- Aadarsh Sahoo, Ankit Singh, Rameswar Panda, Rogerio Feris, and Abir Das. Mitigating dataset imbalance via joint generation and classification. In *ECCV Workshop on Imbalance Problems in Computer Vision*, 2020.
- Dvir Samuel and Gal Chechik. Distributional robustness loss for long-tail learning. *arXiv preprint arXiv:2104.03066*, 2021.
- Florian Schroff, Dmitry Kalenichenko, and James Philbin. Facenet: A unified embedding for face recognition and clustering. In *2015 IEEE Conference on Computer Vision and Pattern Recognition (CVPR)*, pages 815–823, 2015. doi: 10.1109/CVPR.2015.7298682.
- Kihyuk Sohn. Improved deep metric learning with multi-class n-pair loss objective. In D. Lee, M. Sugiyama, U. Luxburg, I. Guyon, and R. Garnett, editors, *Advances in Neural Information Processing Systems*, volume 29. Curran Associates, Inc., 2016.
- Yi Sun, Yuheng Chen, Xiaogang Wang, and Xiaoou Tang. Deep learning face representation by joint identification-verification. In *Proceedings of the 27th International Conference on Neural Information Processing Systems - Volume 2, NIPS’14*, pages 1988–1996, Cambridge, MA, USA, 2014. MIT Press.
- J. Tan, C. Wang, B. Li, Q. Li, W. Ouyang, C. Yin, and J. Yan. Equalization loss for long-tailed object recognition. In *2020 IEEE/CVF Conference on Computer Vision and Pattern Recognition (CVPR)*, pages 11659–11668, 2020.
- Kaihua Tang, Jianqiang Huang, and Hanwang Zhang. Long-tailed classification by keeping the good and removing the bad momentum causal effect. In *NeurIPS*, 2020.
- Aäron van den Oord, Yazhe Li, and Oriol Vinyals. Representation learning with contrastive predictive coding. *CoRR*, abs/1807.03748, 2018. URL <http://arxiv.org/abs/1807.03748>.
- Laurens van der Maaten and Geoffrey Hinton. Visualizing data using t-sne. *Journal of Machine*

- Learning Research*, 9(86):2579–2605, 2008.
- Grant Van Horn and Pietro Perona. The devil is in the tails: Fine-grained classification in the wild. *arXiv preprint arXiv:1709.01450*, 2017.
- Andreas Veit and Kimberly Wilber. Improving calibration in deep metric learning with cross-example softmax. *CoRR*, abs/2011.08824, 2020. URL <https://arxiv.org/abs/2011.08824>.
- B.C. Wallace, K.Small, C.E. Brodley, and T.A. Trikalinos. Class imbalance, redux. In *Proc. ICDM*, 2011.
- Jiaqi Wang, Wenwei Zhang, Yuhang Zang, Yuhang Cao, Jiangmiao Pang, Tao Gong, Kai Chen, Ziwei Liu, Chen Change Loy, and Dahua Lin. Seesaw loss for long-tailed instance segmentation. In *Proceedings of the IEEE Conference on Computer Vision and Pattern Recognition*, 2021a.
- Peng Wang, Kai Han, Xiu-Shen Wei, Lei Zhang, and Lei Wang. Contrastive learning based hybrid networks for long-tailed image classification. *CoRR*, abs/2103.14267, 2021b.
- Kilian Q. Weinberger and Lawrence K. Saul. Distance metric learning for large margin nearest neighbor classification. *J. Mach. Learn. Res.*, 10:207–244, June 2009. ISSN 1532-4435.
- Yandong Wen, Kaipeng Zhang, Zhifeng Li, and Yu Qiao. A discriminative feature learning approach for deep face recognition. In Bastian Leibe, Jiri Matas, Nicu Sebe, and Max Welling, editors, *Computer Vision – ECCV 2016*, pages 499–515, Cham, 2016. Springer International Publishing. ISBN 978-3-319-46478-7.
- Tong Wu, Qingqiu Huang, Ziwei Liu, Yu Wang, and Dahua Lin. Distribution-balanced loss for multi-label classification in long-tailed datasets. In Andrea Vedaldi, Horst Bischof, Thomas Brox, and Jan-Michael Frahm, editors, *Computer Vision – ECCV 2020*, pages 162–178, Cham, 2020. Springer International Publishing. ISBN 978-3-030-58548-8.
- Zhirong Wu, Yuanjun Xiong, Stella X. Yu, and Dahua Lin. Unsupervised feature learning via non-parametric instance discrimination. In *2018 IEEE/CVF Conference on Computer Vision and Pattern Recognition*, pages 3733–3742, 2018. doi: 10.1109/CVPR.2018.00393.
- Jing-Hao Xue and Peter Hall. Why does rebalancing class-unbalanced data improve auc for linear discriminant analysis? *IEEE Transactions on Pattern Analysis and Machine Intelligence*, 37(5): 1109–1112, 2015. doi: 10.1109/TPAMI.2014.2359660.
- Shanming Yang, Weihong Deng, Mei Wang, Junping Du, and Jiani Hu. Orthogonality loss: Learning discriminative representations for face recognition. *IEEE Transactions on Circuits and Systems for Video Technology*, pages 1–1, 2020.
- Yuzhe Yang and Zhi Xu. Rethinking the value of labels for improving class-imbalanced learning. In H. Larochelle, M. Ranzato, R. Hadsell, M. F. Balcan, and H. Lin, editors, *Advances in Neural Information Processing Systems*, volume 33, pages 19290–19301. Curran Associates, Inc., 2020.
- Han-Jia Ye, Hong-You Chen, De-Chuan Zhan, and Wei-Lun Chao. Identifying and compensating for feature deviation in imbalanced deep learning, 2020.
- Han-Jia Ye, De-Chuan Zhan, and Wei-Lun Chao. Procrustean training for imbalanced deep learning. *CoRR*, abs/2104.01769, 2021. URL <https://arxiv.org/abs/2104.01769>.
- Xi Yin, Xiang Yu, Kihyuk Sohn, Xiaoming Liu, and Manmohan Chandraker. Feature transfer learning for face recognition with under-represented data. In *Proceedings of the IEEE/CVF Conference on Computer Vision and Pattern Recognition (CVPR)*, June 2019.
- Junjie Zhang, Lingqiao Liu, Peng Wang, and Chunhua Shen. To balance or not to balance: A simple-yet-effective approach for learning with long-tailed distributions, 2019.
- Songyang Zhang, Zeming Li, Shipeng Yan, Xuming He, and Jian Sun. Distribution alignment: A unified framework for long-tail visual recognition. In *CVPR*, 2021.
- X. Zhang, Z. Fang, Y. Wen, Z. Li, and Y. Qiao. Range loss for deep face recognition with long-tailed

- training data. In *2017 IEEE International Conference on Computer Vision (ICCV)*, pages 5419–5428, 2017.
- Xu Zhang, Felix X. Yu, Sanjiv Kumar, and Shih-Fu Chang. Learning spread-out local feature descriptors. In *2017 IEEE International Conference on Computer Vision (ICCV)*, pages 4605–4613, 2017.
- Yaoyao Zhong, Weihong Deng, Mei Wang, Jiani Hu, Jianteng Peng, Xunqiang Tao, and Yaohai Huang. Unequal-training for deep face recognition with long-tailed noisy data. In *Proceedings of the IEEE/CVF Conference on Computer Vision and Pattern Recognition (CVPR)*, June 2019.
- Dengyong Zhou, Jason Weston, Arthur Gretton, Olivier Bousquet, and Bernhard Schölkopf. Ranking on data manifolds. In *Proceedings of the 16th International Conference on Neural Information Processing Systems, NIPS'03*, page 169–176, Cambridge, MA, USA, 2003. MIT Press.

ELM: Embedding and Logit Margins for Long-Tail Learning

Supplementary Material

A Experiment setup: hyperparameters

A.1 Architecture and optimisation hyperparameters

To facilitate a fair comparison, we use the same setup for all the methods for each dataset. These settings are summarised in Table 3.

For CIFAR, we use the standard CIFAR data augmentation procedure used in previous works such as Cao et al. [2019], He et al. [2016], where 4 pixels are padded on each size and a random 32×32 crop is taken. Images are horizontally flipped with a probability of 0.5. For ImageNet and iNaturalist, we apply the standard data augmentation comprising of random cropping and flipping as described in Goyal et al. [2017].

	CIFAR*-LT	ImageNet-LT	iNaturalist
Model	CIFAR ResNet-32	ResNet-50	ResNet-50
Optimiser	SGD with momentum		
Base learning rate	0.4		
Epochs	256	90	90
Batch size	128	512	1024
Schedule	Linear warmup for the first 15 epochs, and a decay of 0.1 at the 96th, 192nd, and 224th epoch	Cosine	Cosine
Weight decay	10^{-4}	5×10^{-4}	10^{-4}

Table 3: Summary of hyperparameters.

A.2 Settings for ELM

We detail hyperparameter settings for the proposed ELM. For all the four datasets considered in §5, we set the pull margin to be $\alpha_y \propto \mathbb{P}(y)^a$ for some $a > 0$. This choice allows the ELM to pull embeddings of tail classes more strongly compared to frequent classes. Empirically we found that setting $a = \frac{1}{2}$ or $a = 1$ works well for most datasets.

CIFAR10-LT : We use $\alpha_y = \mathbb{P}(y)$, and set the regularization parameter $\lambda = 0.01$.

CIFAR100-LT : We set $\alpha_y = \sqrt{n_y}$, and regularization parameter $\lambda = 0.01$ (see (4)), where n_y denotes the number of training samples in class y .

ImageNet-LT : We set $\alpha_y = 10 \times \sqrt{\mathbb{P}(y)}$ and $\lambda = 0.001$.

iNaturalist : We set $\alpha_y = \sqrt{n_y}$, and set $\lambda = 0.01$.

Based on our investigation, the choice $\alpha_y = n_y$ with $\lambda = 0.01$ appears to offer good performance across many datasets. See also §B.2 where we show how various choices of α_y and λ affect the test accuracy of ELM.

B Experiments: additional results

B.1 Additional margin distributions

Figure 6 plots the cumulative margin distributions ($\gamma(x, y) \doteq f_y(x) - \max_{y' \neq y} f_{y'}(x)$ for instances x with label y) for various methods on CIFAR100-LT. Here, we clearly see a significant gap between ERM and method that enforce a logit margin, which are in turn bested with those that enforce an embedding margin.

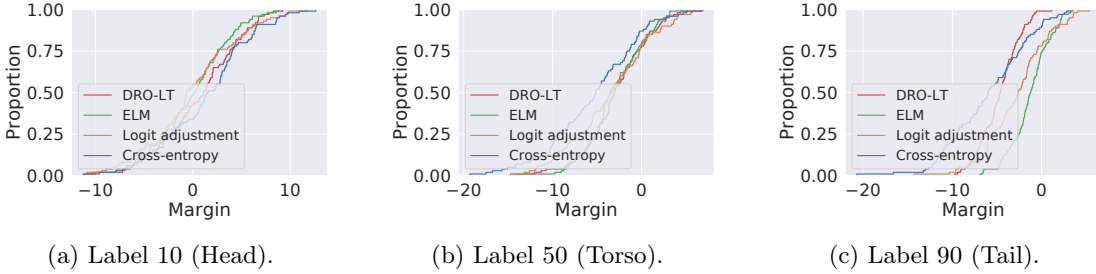


Figure 6: Margin CDF plots on CIFAR100-LT. For a given label y , we plot the cumulative distribution of the margins $\gamma(x, y) \doteq f_y(x) - \max_{y' \neq y} f_{y'}(x)$ for instances x with label y . Logit adjustment is seen to shift margins favourably on the tail label, at some expense on head labels. ELM is seen to consistently reduce the variance of the margin distribution.

B.2 Sensitivity to Regularisation Strength

Figure 7 shows how the choice of regularisation strength λ affects final test set performance of ELM. When λ is too large, performance suffers considerably; when λ is too small, performance is indistinguishable from that of standard cross-entropy minimisation. However, for intermediate values of λ we see some gains, indicating the value of the regulariser.

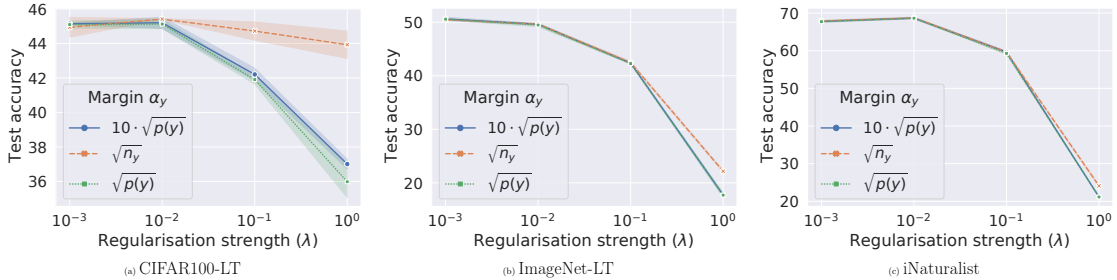


Figure 7: Impact of choice of λ on final balanced accuracy. When λ is too large, performance is seen to suffer; however, an intermediate choice yields gains over standard cross entropy minimisation.

C Proof

C.1 Proof of Proposition 1

We start with the definition of $\Omega_{\text{pull}}(x, y)$:

$$\begin{aligned}
\Omega_{\text{pull}}(x, y) &= \log \left[1 + \sum_{x^+ \in S_y \setminus \{x\}} e^{\|\Phi(x) - \Phi(x^+)\|^2 - \alpha_y} \right] \\
&= \log \left[\frac{1}{|S_y| - 1} \sum_{x^+ \in S_y \setminus \{x\}} 1 + \frac{1}{|S_y| - 1} \sum_{x^+ \in S_y \setminus \{x\}} (|S_y| - 1) e^{\|\Phi(x) - \Phi(x^+)\|^2 - \alpha_y} \right] \\
&\stackrel{(a)}{\geq} \frac{1}{|S_y| - 1} \sum_{x^+ \in S_y \setminus \{x\}} \log \left[1 + (|S_y| - 1) e^{\|\Phi(x) - \Phi(x^+)\|^2 - \alpha_y} \right] \\
&\geq \frac{1}{|S_y| - 1} \sum_{x^+ \in S_y \setminus \{x\}} \log \left[(|S_y| - 1) e^{\|\Phi(x) - \Phi(x^+)\|^2 - \alpha_y} \right] \\
&= \frac{1}{|S_y| - 1} \sum_{x^+ \in S_y \setminus \{x\}} \|\Phi(x) - \Phi(x^+)\|^2 - \alpha_y + \log(|S_y| - 1),
\end{aligned}$$

where at (a) we use Jensen's inequality i.e., $\log\left(\frac{1}{m} \sum_{i=1}^m f(x_i)\right) \geq \frac{1}{m} \sum_{i=1}^m \log(f(x_i))$. This implies that

$$\begin{aligned}
\bar{\Omega}_{\text{pull}}(y) &= \frac{1}{|S_y|} \sum_{x \in S_y} \Omega_{\text{pull}}(x, y) \\
&\geq \frac{1}{|S_y|(|S_y| - 1)} \sum_{x \in S_y} \sum_{x^+ \in S_y \setminus \{x\}} \|\Phi(x) - \Phi(x^+)\|^2 - \alpha_y + \log(|S_y| - 1) \\
&= \frac{1}{|S_y|(|S_y| - 1)} \sum_{x, x^+ \in S_y} \|\Phi(x) - \Phi(x^+)\|^2 - \alpha_y + \log(|S_y| - 1),
\end{aligned}$$

where the last line follows from the fact that $\|\Phi(x) - \Phi(x)\|^2 = 0$.

Observe that $\frac{1}{|S_y|^2} \sum_{x, x^+ \in S_y} \|\Phi(x) - \Phi(x^+)\|^2 = \frac{2}{|S_y|} \sum_{x \in S_y} \|\Phi(x) - \hat{\mu}_y\|^2$ where $\hat{\mu}_y = \frac{1}{|S_y|} \sum_{x \in S_y} \Phi(x)$. To show this, we will start by expanding the square in $\frac{2}{|S_y|} \sum_{x \in S_y} \|\Phi(x) - \hat{\mu}_y\|^2$. In the following derivation, it is useful to note that $\frac{1}{|S_y|} \sum_{x \in S_y} 1 = 1$ is used in many steps, and that $\frac{1}{|S_y|} \sum_{x \in S_y} 1$ is introduced for the purpose of rearranging the expression into a form that has two nested sums:

$$\begin{aligned}
&\frac{2}{|S_y|} \sum_{x \in S_y} \|\Phi(x) - \hat{\mu}_y\|^2 \\
&= \frac{2}{|S_y|} \sum_{x \in S_y} [\|\Phi(x)\|^2 + \|\hat{\mu}_y\|^2 - 2\Phi(x)^\top \hat{\mu}_y] \\
&= \frac{2}{|S_y|} \sum_{x \in S_y} \|\Phi(x)\|^2 + 2 \left\| \frac{1}{|S_y|} \sum_{x \in S_y} \Phi(x) \right\|^2 - \frac{4}{|S_y|} \sum_{x \in S_y} \Phi(x)^\top \left(\frac{1}{|S_y|} \sum_{x^+ \in S_y} \Phi(x^+) \right) \\
&= \frac{2}{|S_y|^2} \sum_{x, x^+ \in S_y} \|\Phi(x)\|^2 + 2 \left(\frac{1}{|S_y|} \sum_{x \in S_y} \Phi(x) \right)^\top \left(\frac{1}{|S_y|} \sum_{x' \in S_y} \Phi(x') \right) - \frac{4}{|S_y|} \sum_{x \in S_y} \Phi(x)^\top \left(\frac{1}{|S_y|} \sum_{x^+ \in S_y} \Phi(x^+) \right)
\end{aligned}$$

$$\begin{aligned}
&= \frac{2}{|S_y|^2} \sum_{x, x^+ \in S_y} \|\Phi(x)\|^2 + \frac{2}{|S_y|^2} \sum_{x, x^+ \in S_y} \Phi(x)^\top \Phi(x^+) - \frac{4}{|S_y|^2} \sum_{x, x^+ \in S_y} \Phi(x)^\top \Phi(x^+) \\
&= \frac{2}{|S_y|^2} \sum_{x, x^+ \in S_y} \|\Phi(x)\|^2 - \frac{2}{|S_y|^2} \sum_{x, x^+ \in S_y} \Phi(x)^\top \Phi(x^+) \\
&= \frac{1}{|S_y|^2} \sum_{x, x^+ \in S_y} \|\Phi(x)\|^2 + \frac{1}{|S_y|^2} \sum_{x, x^+ \in S_y} \|\Phi(x^+)\|^2 - \frac{2}{|S_y|^2} \sum_{x, x^+ \in S_y} \Phi(x)^\top \Phi(x^+) \\
&= \frac{1}{|S_y|^2} \sum_{x, x^+ \in S_y} \left[\|\Phi(x)\|^2 + \|\Phi(x^+)\|^2 - 2\Phi(x)^\top \Phi(x^+) \right] \\
&= \frac{1}{|S_y|^2} \sum_{x, x^+ \in S_y} \|\Phi(x) - \Phi(x^+)\|^2.
\end{aligned}$$

It follows that

$$\begin{aligned}
\bar{\Omega}_{\text{pull}}(y) &\geq \frac{2}{(|S_y| - 1)} \sum_{x \in S_y} \|\Phi(x) - \hat{\mu}_y\|^2 - \alpha_y + \log(|S_y| - 1) \\
&= \frac{2|S_y|}{(|S_y| - 1)} \sum_{j=1}^K \frac{1}{|S_y|} \sum_{x \in S_y} (\Phi(x)_j - \hat{\mu}_{y,j})^2 - \alpha_y + \log(|S_y| - 1) \\
&= \frac{2|S_y|}{(|S_y| - 1)} \sum_{j=1}^K \hat{\mathbb{V}}[\Phi_j(x) | y] - \alpha_y + \log(|S_y| - 1).
\end{aligned}$$

C.2 Proof of Proposition 2 (Generalisation Bound)

Before we give proof for Proposition 2, we present a few lemmas (Lemmas 3, 4, and 5) that will be useful later for proving the proposition. We start with Lemma 3, a known result that gives a probabilistic upper bound of the population mean in terms of an empirical variance.

Lemma 3 (Bennett's inequality [Maurer and Pontil, 2009]). *Let Z_1, \dots, Z_n be i.i.d. random variables with values in $[0, B]$ and let $\delta > 0$. Then, with probability at least $1 - \delta$ in (Z_1, \dots, Z_n) ,*

$$\mathbb{E}Z \leq \frac{1}{n} \sum_{i=1}^n Z_i + \sqrt{\frac{2\hat{\mathbb{V}}[Z] \ln 2/\delta}{n}} + \frac{7B \ln 2/\delta}{3(n-1)}.$$

We will use Lemma 3 as the starting point for proving our generalisation bound of the logit-adjusted cross entropy loss. The logit-adjusted cross entropy loss is a special case of the log loss. Lemma 4 states that the variance of the log loss is no larger than the variance of the linear loss. This observation, together with Lemma 5, will provide necessary intermediate steps in our main proof for connecting the variance of the log loss to the proposed pull objective.

Lemma 4. *Let $\ell_{\log}(y, f(x)) := \log(1 + e^{-yf(x)})$ and $\ell_{\text{lin}}(y, f(x)) = -yf(x)$. Then, for any $y \in \{-1, 1\}$, $\mathbb{V}_{x|y}[\ell_{\log}(y, f(x))] \leq \mathbb{V}_{x|y}[\ell_{\text{lin}}(y, f(x))]$.*

Proof. Let $s_y(z) := \log(1 + e^{-yz})$ for $y \in \{-1, 1\}$. Observe that $s'_y(z) = -\frac{ye^{-yz}}{1+e^{-yz}}$ so that $\sup_z |s'_y(z)| \leq 1$. That is, s_y is a 1-Lipschitz function i.e., for any $z, z' \in \mathbb{R}$, $|s_y(z) - s_y(z')| \leq |z - z'|$. By definition of variance, for any real-valued function h ,

$$\begin{aligned}
\mathbb{V}[h(z)] &= \mathbb{E}[h^2(z)] - \mathbb{E}^2[h(z)] \\
&\leq \mathbb{E}[h^2(z)].
\end{aligned}$$

It follows that

$$\begin{aligned}
\mathbb{V}_{x|y}[\ell_{\log}(y, f(x))] &= \mathbb{V}_{x|y}[s_y(f(x))] \\
&\stackrel{(a)}{=} \mathbb{V}_{x|y}[s_y(f(x)) - s_y(\mathbb{E}_{x'|y}[f(x')])] \\
&\leq \mathbb{E}_{x|y} \left[(s_y(f(x)) - s_y(\mathbb{E}_{x'|y}[f(x')]))^2 \right] \\
&\stackrel{(b)}{\leq} \mathbb{E}_{x|y} \left[(f(x) - \mathbb{E}_{x'|y}[f(x')])^2 \right] \\
&= \mathbb{E}_{x|y} \left[(yf(x) - \mathbb{E}_{x'|y}[yf(x')])^2 \right] \\
&= \mathbb{V}_{x|y}[\ell_{\text{lin}}(y, f(x))],
\end{aligned}$$

where at (a) we note that adding a constant $s_y(\mathbb{E}_{x'|y}[f(x')])$ does not change the variance, and at (b) we use the fact that s_y is 1-Lipschitz. \square

Lemma 5. Consider the binary classification case where $y \in \{-1, 1\}$. Let $f(x) \doteq w^\top \Phi(x) + b \in \mathbb{R}$ be the logit function for class $y = 1$. Define $\Omega_{\text{cen}}(y) := \mathbb{E}_{x|y} \|\Phi(x) - \mu_y\|^2$ where $\mu_y \doteq \mathbb{E}_{x|y} \Phi(x)$. Let $\Omega_{\text{cen}} \doteq \frac{1}{2} [\Omega_{\text{cen}}(-1) + \Omega_{\text{cen}}(1)]$ be the center loss. Then, for any $\Delta_y \in \mathbb{R}$, we have $\mathbb{V}_{x|y}[\ell_{\log}(y, f(x) + \Delta_y)] \leq \|w\|^2 \text{tr}(C_y)$ where $C_y \doteq \mathbb{E}_{x|y} (\Phi(x) - \mu_y)(\Phi(x) - \mu_y)^\top$.

Proof. Let $\lambda_{\max}(A)$ be the the maximum eigenvalue of a square positive definite matrix A . Consider the variance of the linear loss as in Lemma 4. Observe that

$$\begin{aligned}
\mathbb{V}_{x|y}[\ell_{\text{lin}}(y, f(x) + \Delta_y)] &= \mathbb{V}_{x|y}[-y(f(x) + \Delta_y)] \\
&= \mathbb{V}_{x|y}[f(x)] \\
&= w^\top C_y w \\
&\leq \|w\|^2 \|C_y\|_2 \\
&= \|w\|^2 \lambda_{\max}(C_y) \\
&\leq \|w\|^2 \text{tr}(C_y).
\end{aligned} \tag{6}$$

\square

Proof of Proposition 2 We are now ready to prove Proposition 2.

Proof. We first consider the class-conditional logit adjusted loss $\mathbb{E}_{x|y} \ell_{\log}(y, f(x) + \Delta_y)$. For $y \in \{-1, 1\}$, Lemma 3 implies that with probability at least $1 - \delta/2$

$$\mathbb{E}_{x|y} \ell_{\log}(y, f(x) + \Delta_y) \leq \frac{1}{|S_y|} \sum_{x \in S_y} \ell_{\log}(y, f(x) + \Delta_y) + \sqrt{\frac{2\hat{\mathbb{V}}_{x|y}[\ell_{\log}(y, f(x) + \Delta_y)] \ln 4/\delta}{|S_y|}} + \frac{7B \ln 4/\delta}{3(|S_y| - 1)}.$$

As a consequence of the union bound, we have with probability at least $1 - \delta$,

$$\begin{aligned}
&\sum_{y \in \{-1, 1\}} \mathbb{P}(y) \mathbb{E}_{x|y} \ell_{\log}(y, f(x) + \Delta_y) \\
&\leq \sum_{y \in \{-1, 1\}} \mathbb{P}(y) \left[\frac{1}{|S_y|} \sum_{x \in S_y} \ell_{\log}(y, f(x) + \Delta_y) + \sqrt{\frac{2\hat{\mathbb{V}}_{x|y}[\ell_{\log}(y, f(x) + \Delta_y)] \ln 2/\delta}{|S_y|}} + \frac{7B \ln 2/\delta}{3(|S_y| - 1)} \right] \\
&= \sum_{y \in \{-1, 1\}} \frac{\mathbb{P}(y)}{|S_y|} \sum_{x \in S_y} \ell_{\log}(y, f(x) + \Delta_y)
\end{aligned}$$

$$\begin{aligned}
& + \sum_{y \in \{-1,1\}} \mathbb{P}(y) \sqrt{\frac{2\hat{V}_{x|y}[\ell_{\log}(y, f(x) + \Delta_y)] \ln 2/\delta}{|S_y|}} + \frac{7B \ln 2/\delta}{3} \sum_{y \in \{-1,1\}} \frac{\mathbb{P}(y)}{|S_y| - 1} \\
& \doteq T_n + V_n + \frac{7B \ln 2/\delta}{3} \sum_{y \in \{-1,1\}} \frac{\mathbb{P}(y)}{|S_y| - 1} \\
& \doteq (\heartsuit),
\end{aligned}$$

where we define $T_n \doteq \sum_{y \in \{-1,1\}} \frac{\mathbb{P}(y)}{|S_y|} \sum_{x \in S_y} \ell_{\log}(y, f(x) + \Delta_y)$ and $V_n \doteq \sum_{y \in \{-1,1\}} \mathbb{P}(y) \sqrt{\frac{2\hat{V}_{x|y}[\ell_{\log}(y, f(x) + \Delta_y)] \ln 2/\delta}{|S_y|}}$. We upper bound V_n as

$$\begin{aligned}
V_n & \stackrel{(a)}{\leq} \sqrt{\sum_{y \in \{-1,1\}} \frac{2\mathbb{P}(y)}{|S_y|} \hat{V}_{x|y}[\ell_{\log}(y, f(x) + \Delta_y)] \ln 2/\delta} \\
& \stackrel{(b)}{\leq} \sqrt{\ln \frac{2}{\delta} \sum_{y \in \{-1,1\}} \frac{2\mathbb{P}(y)}{|S_y|} \|w\|^2 \text{tr}(\hat{C}_y)} \\
& \doteq (\star)
\end{aligned}$$

where at (a) we use Jensen's inequality, (b) follows from Lemma 5, $\hat{C}_y \doteq \frac{1}{|S_y|} \sum_{x \in S_y} (\Phi(x) - \hat{\mu}_y)(\Phi(x) - \hat{\mu}_y)^\top$, and $\hat{\mu}_y \doteq \frac{1}{|S_y|} \sum_{x \in S_y} \Phi(x)$. By Proposition 1, we have

$$\begin{aligned}
\frac{2|S_y|}{|S_y| - 1} \cdot \text{tr}(\hat{C}_y) - \alpha_y + \log(|S_y| - 1) & \leq \bar{\Omega}_{\text{pull}}(y), \text{ implying that} \\
2\text{tr}(\hat{C}_y) & \leq \bar{\Omega}_{\text{pull}}(y) + \alpha_y - \log(|S_y| - 1) \\
& \leq \bar{\Omega}_{\text{pull}}(y) + \alpha_y.
\end{aligned}$$

The last inequality suggests that

$$V_n \leq (\star) \leq \|w\| \sqrt{\ln \frac{2}{\delta} \sum_{y \in \{-1,1\}} \frac{\mathbb{P}(y)}{|S_y|} [\bar{\Omega}_{\text{pull}}(y) + \alpha_y]}.$$

Combining the last line with () gives the result. \square

D Additional related work

Improved embedding geometry. Several works have studied means of improving the geometry of learned embeddings for classification tasks. The center loss [Wen et al., 2016] pulls sample embeddings towards their class centroid μ_y :

$$\Omega_{\text{center}}(x, y) \doteq \|\Phi(x) - \mu_y\|_2^2.$$

Conversely, several works have studied regularisers that push apart embeddings [Zhang et al., 2017, Hayat et al., 2019, Krichene et al., 2019, Yang et al., 2020]; e.g., under the assumption that embeddings are normalised, the spreadout regulariser [Zhang et al., 2017] is

$$M_1 = \frac{1}{|\{x \neq x'\}|} \sum_{x \neq x'} \Phi(x)^\top \Phi(x') \tag{7}$$

$$M_2 = \frac{1}{|\{x \neq x'\}|} \sum_{x' \neq x} (\Phi(x)^\top \Phi(x'))^2 \tag{8}$$

$$\Omega_{\text{spread}}(x, y) \doteq M_1^2 + \max\left(0, M_2 - \frac{1}{d}\right). \quad (9)$$

Similar regularisers were also explored in a long-tailed setting by [Zhong et al. \[2019\]](#). None of the above techniques consider an explicit margin for their “pull” or “push” regularisation.

Deep LDA. Fisher linear discriminant analysis [[FISHER, 1936](#)] is a classical means of tackling classification, which relies on finding projections that minimise intra-class variance (i.e., pull together projected scores) and maximise inter-class variance (i.e., push apart projected scores). In a deep learning context, [Dorfer et al. \[2015\]](#) proposed a form of deep LDA. This is not attuned to the long-tail setting, and does not enforce classification or embedding margins.